PROCEEDINGS OF SCIENCE

Optimization of spin-coherence time for Electric Dipole Moment measurements in a Storage Ring

Rahul Shankar[a,b,*], **Anna Piccoli**[b], **Paolo Lenisa**[a,b] **and Andreas Lehrach**[c,d]

a Instituto Nazionale di Fisica Nucleare (INFN), Ferrara, Italy

b Università degli studi di Ferrara, Ferrara, Italy

c Forschungszentrum Jülich, 52425 Jülich, Germany

d RWTH Aachen University and JARA-FAME, 52056 Aachen, Germany

E-mail: shankar@fe.infn.it, lenisa@fe.infn.it

On behalf of the JEDI and CPEDM collaborations

Electric dipole moments are very sensitive probes of physics beyond the Standard Model. The JEDI collaboration is dedicated to the search for the electric dipole moment (EDM) of charged particles making use of polarized beams in a storage ring. In order to reach the highest possible sensitivity, a fundamental parameter to be optimized is the Spin Coherence Time (SCT), i.e., the time interval within which the particles of the stored beam maintain a net polarization greater than 1/e. To identify the working conditions that maximize SCT, accurate spin-dynamics simulations have been performed using BMAD. In this study, lattices of a "prototype" storage ring, which uses combined electric and magnetic fields for bending, and a "hybrid" storage ring using only electric bending fields with magnets for focusing, are investigated. This paper presents a model of spin behaviour in frozen-spin lattices that models spin tune with reasonable accuracy in both situations, as well as a technique to optimize the second-order beam optics for maximum SCT at any given working point.

25th International Spin Physics Symposium (SPIN 2023)
24-29 September 2023
Durham, NC, USA

*Speaker

PoS(SPIN2023)092

1 Introduction

Of all the observable matter antimatter asymmetry in the universe only a small fraction is accounted for by the currently accepted Standard Model (SM). Assuming the CPT theorem to hold true, it appears that this asymmetry can only be explained by additional CP violating processes than those accounted for in the SM [1]. A noticeable manifestation of CP violation is the presence of an Electric Dipole Moment in a proton, whose magnitude can indicate the existence of additional CP violation Beyond the Standard Model (BSM). While the SM predicts an EDM $\leq 10^{-31}\ e \cdot cm$, possible contributions from BSM theories could place it orders of magnitude higher. The current upper limit on the proton EDM is $7.9 \times 10^{-25}\ e \cdot cm$ [2].

The JEDI collaboration is currently working on performing this measurement using storage rings. EDM can be measured using a storage ring through precise observation of the interaction of particle spin with electric and magnetic fields. Since the EDM will point in the same direction as the spin, the presence of EDM will result in a torque on the particle in response to an electric field. The visible effect of this torque can be magnified using specially configured external electric fields. To achieve a precision higher than the current lower limit on the proton EDM, the construction of a dedicated storage ring would be needed [3] [4]. But before building such a ring, its feasibility must be demonstrated. So, to this end the JEDI collaboration will approach this problem in three stages [3]. The first stage involves experiments at the Cooler Synchrotron (COSY) in FZ, Jülich, with only magnetic bending fields. The second stage involves experiments in a prototype storage ring which uses a combination of electric and magnetic bending fields, featuring the possibilities of simultaneous counter-rotating beams and frozen spin.

Once the prototype has established the proof-of-principle, the final stage can be initiated, which would involve the measurement of the proton EDM at a purely electric storage ring, which would have the targeted precision to do so.

2 Spin tune and Frozen Spin

In a storage ring that confines particles with anomalous magnetic moment G with a velocity $\vec{v}$ using an electric field $\vec{E}$ and a magnetic field $\vec{B}$ such that the three vectors are mutually perpendicular, the spins of the particles would undergo precession with respect to their velocity vectors due to the presence of a magnetic dipole moment (MDM), and an electric dipole moment (EDM). The frequency of this precession for a particle of mass m and charge q is given by the Thomas BMT equation [5]:

$$\begin{aligned}\frac{d\vec{\boldsymbol{s}}}{dt} &= -\frac{q}{m}\left[\left\{\left[\vec{\Omega}_{MDM}\right]_{rel}\right\} + \left\{\vec{\Omega}_{EDM}\right\}\right] \times \vec{\boldsymbol{s}} \\ &= -\frac{q}{m}\left[\left\{G\vec{B} + \left(G - \frac{1}{\gamma^2 - 1}\right)\vec{v} \times \vec{E}\right\} + \left\{\frac{\eta}{2}\left(\vec{E} + \vec{v} \times \vec{B}\right)\right\}\right] \times \vec{\boldsymbol{s}}\end{aligned} \quad (1)$$

The expression for the precession frequency above allows us to define the "spin tune" (ν_s), which can be understood as the angle of precession of the spin in the particle rest frame (according to the Frenet-Serret Coordinate system) per radian of turn of the particle around the ring. In the case of a pure-magnetic storage ring ($\vec{B} = 0$), $\nu_s = \gamma G$ [6], where γ is the Lorentz factor. However, in the presence of both electric and magnetic fields (but no EDM), it can be shown that:

$$\nu_s = \gamma G - \frac{r(G+1)}{\gamma(\beta + r)} \quad (2)$$

Where $r = {}^{E}/_{cB}$ is the normalized field ratio, and $\beta = {}^{v}/_{c}$.

The values of $\vec{E}$, $\vec{B}$ and γ in eq(1) can be set to make the relative precession due to the MDM ($\left[\vec{\Omega}_{MDM}\right]_{rel}$) vanish altogether, effectively resulting in a zero spin tune. This is called "frozen spin" since in this configuration, the spin vector is aligned with the particle momentum at all times. Therefore, any precession of the particle's spin is now solely due to the EDM, and will be in the vertical plane, causing a gradual build-up of vertical polarization among particles in the ring. The rate of this build-up will be proportional to the magnitude of the particle's EDM. The field ratio to obtain frozen spin can be calculated from eq(2) by setting $\nu_s = 0$:

$$\nu_s = \gamma G - \frac{r(G+1)}{\gamma(\beta + r)} = 0 \quad \Rightarrow \quad r = \frac{\beta\gamma^2 G}{1 - \beta^2\gamma^2 G} \approx 0.7147 \quad (3)$$

3 The Prototype EDM Storage Ring

One such combination of fields respecting eq(3) is implemented for a ring with a bending radius of $12.25\ m$. The proposed design [6], which is the same lattice as used in [8], shown in Figure 1 consists of four unit-cells, each with two bending dipoles, 4 quadrupoles and 4 sextupoles to provide sufficient flexibility in beam optics. The quadrupoles present on the ring are categorized into three families: QF (2 per unit cell, focussing), QD (1 per unit cell, defocussing) and QSS (1 per unit cell, in the straight section). The sextupoles are placed on the same locations as the quadrupoles and are categorized into similar families: SXF, SXD and SXSS. Each family of magnets have a common power supply for centralized control. During this study however, the QSS magnets were turned off. An RF-cavity is also placed at one of the straight sections for bunching (longitudinal focussing) of particles.

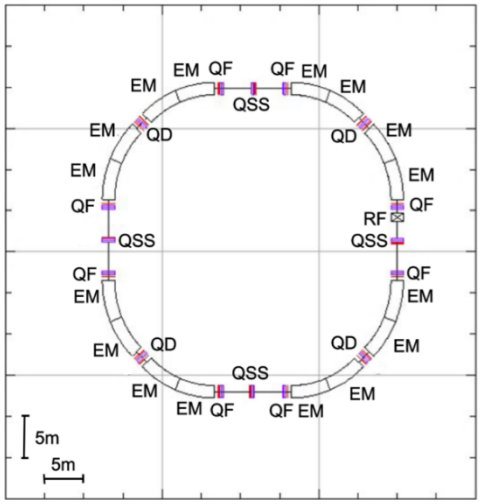

Figure 1: The software generated floor plan of the prototype EDM ring. Dipoles are labelled with 'EM', quadrupoles corresponding to their family with 'QF', 'QD' or 'QSS' and the cavity with 'RF'.

3.1 Spin Tune in a frozen-spin storage ring

3.1.1 RF cavity off

The frozen spin condition fixes the spin tune of its reference particle[1] at zero.

[1] Particle that is following the "reference trajectory" where it maintains its position and momentum at the design-values such that no focusing is required. All phase-space parameters of real particles at any given time are with reference to those of this particle.

However, this is not true for a real particle[2]. Of the six phase-space parameters that a particle exhibits at a given time, the largest contribution to the spin tune comes from the longitudinal momentum offset $\delta = {\Delta p}/{p}$.This can be closely approximated for reasonable perturbations by taking terms up to the second order:

$$\nu_s = \sigma_0 \delta + \sigma_1 \delta^2 \quad (4)$$

While these "spin-tune factors" σ_0 and σ_1 (first and second order respectively) can be calculated directly from eq(2), in a ring where the particle assumes relativistic speeds, the effects of phase slip have been shown to affect the values of these constants. Furthermore, the presence of quadrupoles in the ring have been observed to affect the spin tune. This contribution would depend on the transverse emittances of the particle. Finally, the presence of chromaticity in the ring have also been shown to produce an additional contribution to the spin tunes of particles with non-zero emittances through modifications to the path length [9]. Taking all these factors into consideration, and including the effects of phase-slip up to the second order, the spin tune of a particle in a frozen-spin storage ring can be modelled as follows:

$$\nu_s = \sigma_0 \delta + \epsilon_i a^i + \epsilon_i V^i{}_j \xi^j \quad (5)$$

Here, the indices $i, j \in \{1,2,3\}$, and the Einstein summation convention is followed for repeated indices. The arrays ϵ_i and ξ^j are assigned as follows:

$$[\epsilon_i] = \begin{bmatrix} \epsilon_x & \epsilon_y & \delta^2 \end{bmatrix} \quad [\xi^j] = \begin{bmatrix} \xi_x \\ \xi_y \\ \eta_1 \end{bmatrix} \quad (6)$$

…where ϵ_x and ϵ_y are the horizontal and vertical emittances, ξ_x and ξ_y are the horizontal and vertical chromaticities, and η_1 is the second-order phase-slip factor. The three parameters arranged in the vector a^i and the nine matrix elements $V^i{}_j$ are free parameters which set the strengths/couplings of the respective contributions to the spin tune.

In this study, single-particle simulations were performed, and simultaneous least-square fitting was done over a large sample-space to accurately determine these parameters, and the predictions were compared to measurements of more samples to test the validity of the model.

3.1.2 Travel time

The change in travel time in longitudinal beam dynamics is modeled as:

$$\frac{\Delta t}{t} = \eta_0 \delta + \eta_1 \delta^2 \quad (7)$$

However, it is also known that the presence of chromaticity in the ring affects the path length of particles with non-zero transverse emittances [9]…

$$\left(\frac{\Delta L}{L}\right)_\beta = -\frac{\pi}{L}\left(\epsilon_x \xi_x + \epsilon_y \xi_y\right) \quad (8)$$

…which could in turn influence the travel time. Thus, putting together the transverse and longitudinal contributions, the change in travel time can be modeled in a similar fashion as the spin tune:

[2] Particle that is not following the reference trajectory, i.e., having non-zero phase space parameters w.r.t the reference particle.

$$\frac{\Delta t}{t} = \eta_0 \delta + \epsilon_i T^i{}_j \xi^j \quad (9)$$

3.1.3 RF cavity on

The RF cavity, used to provide longitudinal bunching in storage rings, induces longitudinal oscillations on the particle, known as synchrotron oscillations. This changes the nature of the phase-space parameter δ, thus needing a reconsideration of the way the spin tune is dealt with.

$$\delta = \langle\delta\rangle + \delta_a \, sin(\omega_s \phi + \varphi_0) \quad (10)$$

Here, $\langle\delta\rangle$ is the net momentum gained by the particle from the cavity, and δ_a and ω_s are the amplitude and frequency of the synchrotron oscillations.

In the absence of longitudinal focusing, the particle's momentum is (ideally) fixed, usually leading to the observation of a constant spin tune. However, in the presence of longitudinal focusing, the variation of δ leads to an oscillation of the spin along with the particle, resulting in an oscillating spin tune. The quantity of interest now would be the time-averaged spin tune $\langle\nu_s\rangle$, where the pointy brackets $\langle \quad \rangle$ represent an averaging over many synchrotron oscillations.

Averaging eq(10) over many synchrotron oscillations allows the evaluation of $\langle\delta^2\rangle$:

$$\langle\delta^2\rangle = \langle\delta\rangle^2 + \frac{\delta_a^2}{2} \approx \frac{\delta_a^2}{2} \quad (11)$$

Finally, the boundary condition for longitudinal focusing [10] can be applied, i.e., the synchrotron-averaged change in travel time must vanish. From eq(9):

$$\left\langle\frac{\Delta T}{T}\right\rangle = \eta_0\langle\delta\rangle + \langle\epsilon\rangle_i T^i{}_j \xi^j = 0 \quad \Rightarrow \quad \langle\delta\rangle = -\frac{1}{\eta_0}\langle\epsilon\rangle_i T^i{}_j \xi^j \quad (12)$$

This condition allows for the elimination of the $\langle\delta\rangle$ term in the final expression for $\langle\nu_s\rangle$, resulting in the following expression for the synchrotron-averaged spin tune of a particle:

$$\langle\nu_s\rangle = \langle\epsilon\rangle_i a^i + \langle\epsilon\rangle_i M^i{}_j \xi^j \quad (13)$$

…where:

$$\begin{aligned} M^i{}_j &= V^i{}_j - \frac{\sigma_0}{\eta_0} T^i{}_j \\ [\langle\epsilon\rangle_i] &= \begin{bmatrix} \epsilon_x & \epsilon_y & \frac{\delta_a^2}{2} \end{bmatrix} \end{aligned} \quad (14)$$

3.2 Linear map from sextupole settings to chromaticity and second-order phase slip

It was observed that there exists a linear map between the sextupole field strengths and the chromaticities. Therefore, if a lattice has two functioning families of sextupoles, the horizontal and vertical chromaticities can be simultaneously set.

$$\begin{aligned} \xi_x &= \xi_{x_0} + X_{11} t_1 + X_{12} t_2 \\ \xi_y &= \xi_{y_0} + X_{21} t_1 + X_{22} t_2 \end{aligned} \quad (15)$$

…where ξ_{x_0} and ξ_{y_0} are the natural chromaticities[3], and $t_{1,2}$ are the sextupole field strengths. Furthermore, since the second order phase-slip factor can also be set via sextupole settings in a similar way,

$$\eta_1 = \eta_{1_0} + X_{31} t_1 + X_{32} t_2 \quad (16)$$

[3] The chromaticity present in the ring by default, when the sextupoles are turned off.

…having three sextupole families would enable the access of any configuration of the three second-order optical parameters that determine the spin tune.

$$\xi^i = {\xi_0}^i + {X^i}_j t^j \quad (17)$$

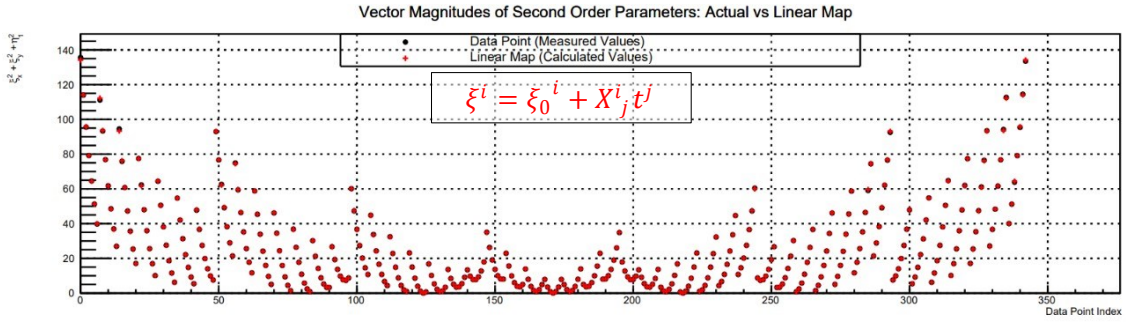

Figure 2: A plot comparing the values of $\xi_i \xi^i$ as measured by BMAD at the sample sextupole setting and as predicted by the linear map of eq(17). A perfect overlap of the points would signify that the model is an accurate representation of (simulated) reality.

This linear map, when combined with three families of sextupoles present in the lattice, allows access to the entire domain of the spin tune (full optical flexibility).

Using the three sextupole families present in the prototype ring, the matrix elements ${X^i}_j$ were determined and used to determine the optical parameters ξ^i for a regular grid of sample sextupole settings. These calculated values were then compared with the measurements of ξ^i done by BMAD. The result of this comparison is shown in Figure 2.

4 Results and Discussion

4.1 RF off

A large sample set of points, each representing a particle with a particular ϵ_x, ϵ_y and δ, being simulated in a ring with a particular combination of ξ_x, ξ_y and η_1, was used to determine the constants in eq(5). Once determined, the model was used to determine spin tunes for a new set of sample points. The comparison of these calculated values and those measured by BMAD at those points is shown in Figure 3.

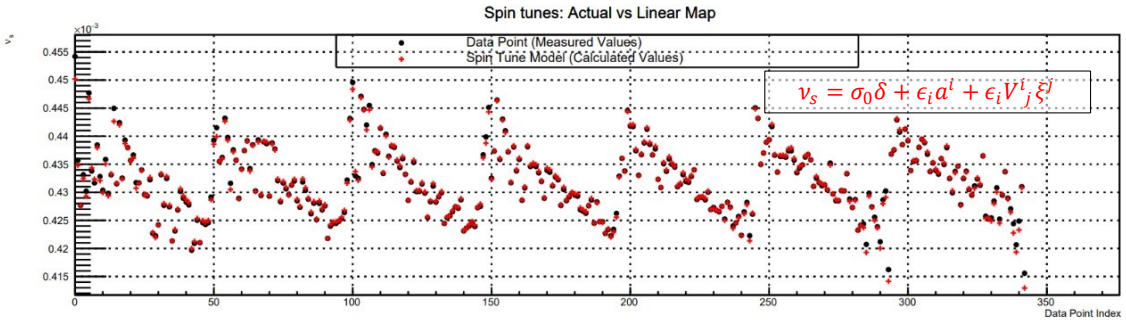

Figure 3: A plot comparing the spin tunes as measured by BMAD and those determined by the spin tune model of eq(5).

A similar determination of constants and subsequent testing was done with the change in travel time $\left(\frac{\Delta t}{t}\right)$. This is shown in Figure 4.

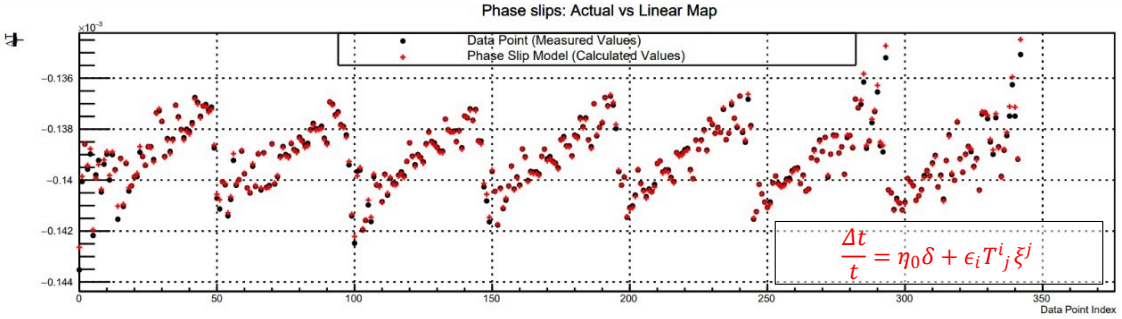

Figure 4: A plot comparing the spin tunes as measured by BMAD and those determined by the spin tune model of eq(5).

A perfect alignment of the data points with one-another in these comparisons would imply that the model exactly reflects the variation of the spin tune or travel time by the simulator. However, slight misalignments were observed between the measured and calculated values. It is also interesting to observe the similarity in the variations of the spin tune and the change in travel time. The close correlation between the two also adds merit to the mechanism of changes in travel time due to phase-slip being the primary force behind changes in spin tune.

4.2 RF on

Using the spin tune model optimized for the RF cavity being on (eq(13) and eq(14)), a sample set of points were simulated again, but this time with the RF cavity on. The result of the comparison of the measured time-averaged spin tune with those predicted by the model is shown in Figure 5.

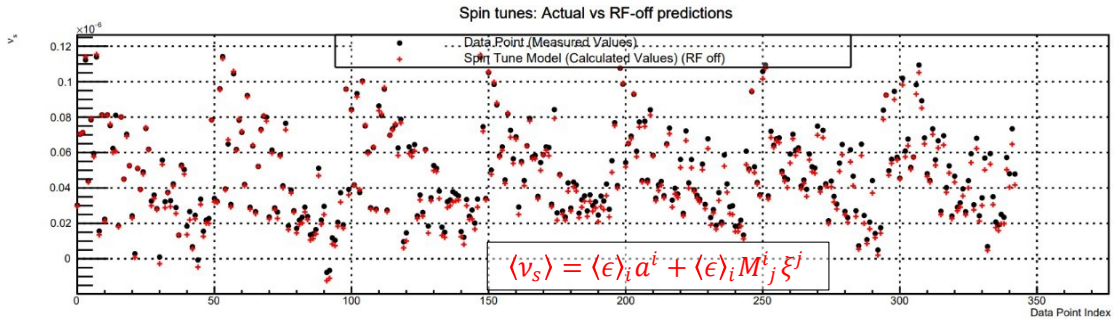

Figure 5: A plot comparing the spin tunes as measured by BMAD and those determined by the spin tune model of eq(13) for a storage ring with longitudinal focusing.

While the model shows decent agreement with the findings, the increased misalignment between the measured and predicted values is a matter of concern. To better understand the reasons for this increased misalignment, the constants a^i and $M^i{}_j$ were redetermined using a sample set similar to the one used before, but this time where the particles are simulated with longitudinal focusing turned on. The model, now updated with the newly determined constants, was tested again with a fresh set of sample points, whose results are shown in Figure 6.

As can be seen from the plot, the predictions now align perfectly with the measurements. This suggests that while the RF-on model accurately reflects spin behavior in the storage ring, the process of determining the constants with the RF off and using them to estimate those in the RF-on model may also allow for the propagation of errors. Moreover, the higher disparity in the RF-

off result (Figure 3) than in the RF-on case (Figure 6) also points toward systematic errors in the RF-off optimization process.

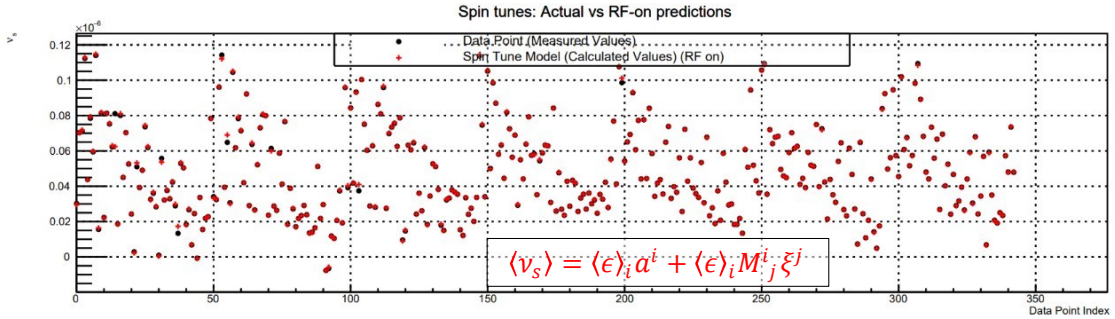

Figure 6: A plot comparing the spin tunes as measured by BMAD and those determined by the spin tune model of eq(13), updated with constants determined while the longitudinal focusing was on.

4.3 Importance of modelling spin tune in optimization of Spin Coherence Time

In [8], the measurement and optimization of Spin Coherence Time is discussed in detail. Here, essentially a brute-force method is implemented where SCT is measured using simulations of bunches rather than individual particles. While this method is highly accurate, it unfortunately demands a lot of time and computing power to carry out.

However, accurate spin-tune modelling can remove the need for such large-scale simulations. If eq(13) were re-written as…

$$\langle \nu_s \rangle = \langle \epsilon \rangle_i \left(a^i + M^i{}_j \xi^j \right) \qquad (18)$$

…it is intuitive to understand that there can exist a particular optical setting such that:

$$a^i + M^i{}_j \xi^j = 0 \qquad (19)$$

In such a setting, it is clear that the time averaged spin tune of a particle would essentially be zero regardless of its emittance or momentum offset amplitude. A many-particle bunch being simultaneously stored in a storage ring is simply particles with different $\langle \epsilon \rangle_i$ being subject to the same special optical setting ξ^j. Therefore, it can be seen that in principle, all the particles in the bunch should exhibit close to zero spin tune and so the bunch as a whole would have a very high spin coherence time.

Given that the model be highly accurate, this special setting is simply estimated by:

$$\xi^j = -(M^{-1})^j{}_i a^i \qquad (20)$$

This way the optimized point can be determined through single particle simulations alone.

5 Conclusions

In this paper, a model of the spin tune of a single particle stored in a prototype storage ring that achieves frozen spin using a combination of electric and magnetic fields is described. The model predicts the spin tune not only at various settings of the prototype ring but also at other frozen-spin lattices, such as a modified prototype and also the Hybrid Storage Ring [11] with a reasonable accuracy. The model was tested extensively with the prototype ring and the degree of accuracy in predicting spin behaviour achieved so far have been presented.

While the method to optimize spin coherence time was attempted at a few working points, the field settings of the optimized point as determined by the model were close to those already measured using brute force, but not close enough to exhibit spin coherence times higher than 1000

seconds. As concluded from previous works [8] [12], the optimized setting for SCTs higher than 1000s is highly sensitive to the sextupole settings. To be able to determine this from the single-particle model demands a much higher precision from the model. This is currently the primary focus of this ongoing work.

6 References

[1] A. Sakharov, «Violation of CP invariance, C asymmetry, and baryon asymmetry of the universe,» *JETP Letters,* vol. 5, pp. 24-27, 1967.

[2] V F Dmitriev e R A Sen'kov, «Schiff Moment of the Mercury Nucleus and the Proton Dipole Moment,» *Physical Review Letters,* vol. 91, p. 212303, 2003.

[3] CPEDM Collaboration, «Storage ring to search for electric dipole moments for charged particles: Feasibility study,» CERN Yellow Reports: Monographs, Geneva, 2021.

[4] P. Lenisa, «Search for Electric Dipole Moments of Charged Particles with Polarized Beams in Storage Rings,» in *The 18th International Workshop on Polarized Sources, Targets, and Polarimetry*, Knoxville, 2019.

[5] V. Bargmann, L. Michel e V.L. Telegdi, «Precession of the polarization of particles moving in a homogeneous electromagnetic field,» *Physical Review Letters,* vol. 2, n. 10, p. 435, 1959.

[6] S Y Lee, Accelerator Physics (Fourth Edition), Singapore: World Scientific, 2019.

[7] A Lehrach, S Martin e R Talman, «Design of a Prototype EDM Storage Ring,» in *23rd International Spin Physics Symposium*, Ferrara, 2018.

[8] R. Shankar, P. Lenisa e A. Lehrach, «Optimization of spin-coherence time for electric dipole moment measurements,» in *19th Workshop on Polarized Sources, Targets and Polarimetry (PSTP2022)*, Mainz, Germany, 2022.

[9] Yoshihiko Shoji, «Dependence of average path length betatron motion in a storage ring,» *Physical Review Special Topics - Accelerators and Beams,* vol. 8, p. 094001, 2005.

[10] Marcel Stephan Rosenthal, «Experimental Benchmarking of Spin Tracking Algorithms for Electric Dipole Moment Searches at the Cooler Synchrotron COSY,» PhD Thesis, RWTH Aachen University, Aachen, 2016.

[11] Z. Omarov, H. Davoudiasl e et. al., «Comprehensive Symmetric-Hybrid ring design for a pEDM experiment at below 10^-19 e.cm,» *Physical Review D,* n. 032001, p. 105, 2021.

[12] R. Shankar, M. Vitz e P. Lenisa, «Optimization of Spin Coherence Time at a Prototype Storage Ring for Electric Dipole Moment Measurements,» in *24th International Spin Symposium (SPIN2021)*, Matsue, 2022.

[13] G Guidoboni, E J Stephenson, A Wrońska e et. al., «Connection between zero chromaticity and long in-plane polarization lifetime in a magnetic storage ring,» *Physical review accelerators and beams,* vol. 21, p. 024201, 2018.